ACS APPLIED MATERIALS & INTERFACES

Research Article

www.acsami.org

Killing Dental Pathogens Using Antibacterial Graphene Oxide

Jianliang He,[†,‡] Xiaodan Zhu,[†,‡] Zhengnan Qi,[‡] Chang Wang,[‡] Xiaojun Mao,[‡] Cailian Zhu,[§] Zhiyan He,[§] Mingyu Li,[§] and Zisheng Tang*[,‡]

[‡]Department of Endodontics, Ninth People's Hospital, School of Medicine, Shanghai Key Laboratory of Stomatology, and [§]Shanghai Research Institute of Stomatology, Ninth People's Hospital, School of Medicine, Shanghai Jiao Tong University, 639 ZhiZaoJu Road, Shanghai 200011, People's Republic of China

ABSTRACT: Dental caries and periodontal diseases have a close relationship with microbes such as *Streptococcus mutans*, *Porphyromonas gingivalis* and *Fusobacterium nucleatum*. Graphene oxide (GO), as the derivative of graphene, plays an important role in many areas including biology and medicine. In particular, it has been known as a promising antimicrobial nanomaterial. In this study, we focused on the antimicrobial property of GO against dental pathogens. With the utilization of 3-(4,5-dimethylthiazol-2-yl)-2,5-diphenyl tetrazolium bromide (MTT) reduced test, colony forming units (CFU) counting, growth curve observation, live/dead fluorescent staining, and confocal laser scanning microscopy (CLSM), we found GO nanosheets were highly effective in inhibiting the growth of dental pathogens. Transmission electron microscopy (TEM) images revealed that the cell wall and membrane of bacteria lost their integrity and the intracellular contents leaked out after they were treated by GO. Therefore, GO nanosheets would be an effective antibacterial material against dental pathogens and the potential applications in dental care and therapy are promising.

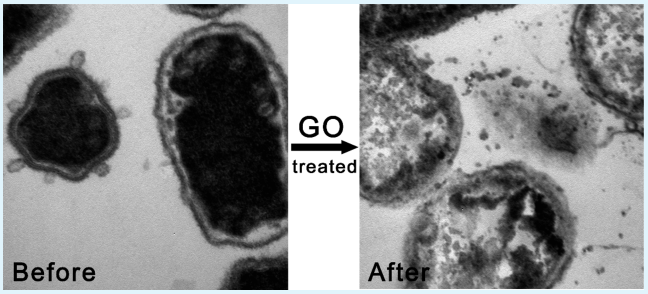

KEYWORDS: *graphene oxide, dental pathogens, antibacterial material, Streptococcus mutans, Fusobacterium nucleatum, Porphyromonas gingivalis*

1. INTRODUCTION

Dental caries and periodontal diseases have a close relationship with microbes. Oral microbial colonization exists in a balance with microenvironment in oral.[1] Adverse reactions arise if the balance got out of order. *Streptococcus mutans* is Gram-positive, facultative anaerobic, and an important cariogenic microorganisms.[2] *S. mutans* produces large amounts of organic acids, which leads to a decrease in the pH value of the microenvironment of the oral cavity. *Porphyromonas gingivalis* and *Fusobacterium nucleatum* are all Gram-negative anaerobic bacteria, which are associated with periodontitis[3,4] and root canal infection.[5]

Graphene, an allotropic type of carbon, was first successfully prepared by Geim and Novoselov in 2004.[6] Graphene is constituted of single-atom-thick carbon nanosheets with a honeycomb structure.[7] Graphene oxide is a derivative of graphene which is modified by a number of oxygen-containing groups on the graphene sheet, such as carboxyl, epoxy, carbonyl, hydroxyl, etc. Because of these groups, highly conjugated graphene structure is damaged. However, at the same time, GO nanosheets has a better chemical stability and solubility in water.[8] Graphene and graphene oxide are recognized as promising nanomaterial to be applied in biologic and medical fields. So far, based on a few reports, it is noted that graphene, graphene oxide and reduced graphene oxide suspensions can inhibit the growth of *Escherichia coli*, *Staphylococcus aureus*, *Bacillus subtilis*, etc., however, with a minimal cytotoxicity.[9−13] The effects of graphene oxide against more dental pathogens need to be explored.

In this study, we used three typical bacteria of dental caries, periodontal, and periapical diseases, *S. mutans*, *P. gingivalis* and *F. nucleatum*, to evaluate the antibacterial activity of GO nanosheets in different concentrations. MTT reduced assay, CFU counting method, growth curves observation, and live/dead fluorescent staining were applied to confirm whether GO nanosheets worked. Transmission electron microscopy (TEM) technique was used to reveal the change of bacterial cells in ultramicroscopic dimension.

2. MATERIALS AND METHODS

2.1. Preparation and Characterization of Graphene Oxide. The modified Hummers' method was utilized to prepare graphene oxide from natural graphite as described in previous work.[9,14,15] We employed atom force microscopy (AFM, Nanoscope IIIa,USA) to detect the morphology and size of GO, and used dynamic light scattering (DLS, Thermo, USA) to analyze GO' hydrodynamic diameters and size distribution. We further investigated the surface functional groups on GO and carbons structure of GO using Fourier transform infrared spectroscopy (FTIR, Thermo, USA) and Raman spectroscopy (XPLORA INV), respectively.

Received: February 3, 2015
Accepted: February 23, 2015
Published: February 23, 2015

DOI: 10.1021/acsami.5b01069
ACS Appl. Mater. Interfaces 2015, 7, 5605−5611

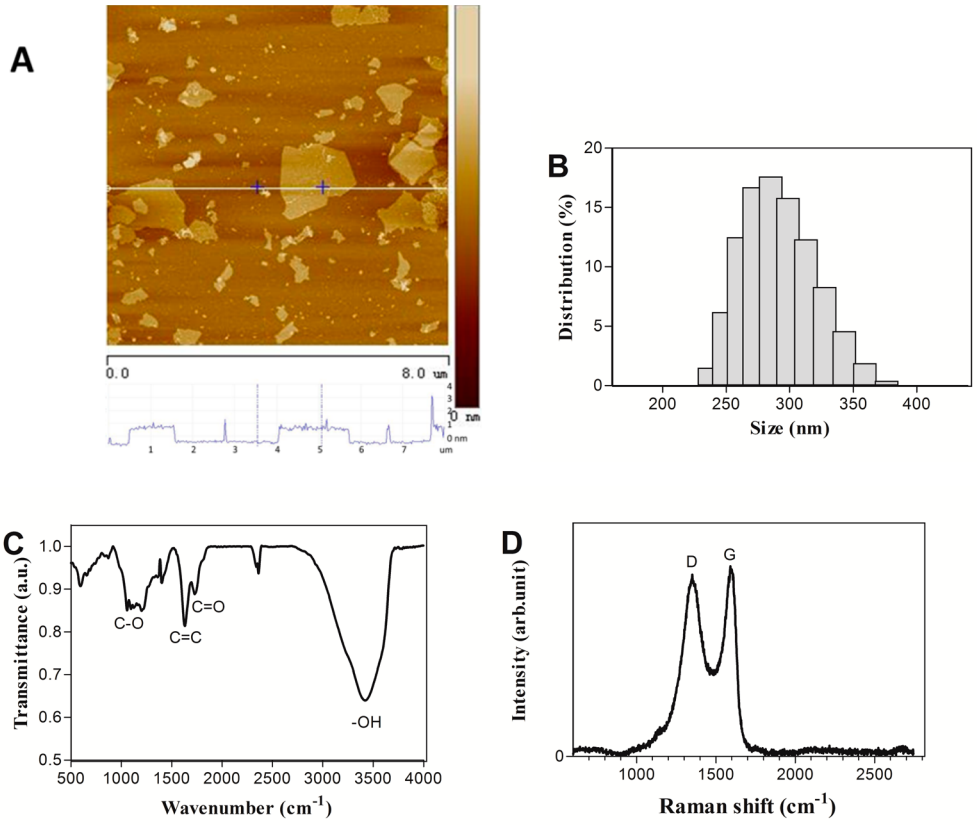

Figure 1. Characterization of graphene oxide. (A) Atom force microscopy image of GO. (B) Hydrodynamic diameters and size distribution of GO. (C) FT-IR spectrum and (D) Raman spectrum of GO.

2.2. Bacterial Strains and Culture Conditions. Oral microoganism strains, *S. mutans* (UA159), *F. nucleatum* (ATCC 10953) and *P. gingivalis* (ATCC 33277) were obtained from Shanghai Key Laboratory of Stomatology, Ninth People's Hospital, Shanghai Jiao Tong University School of Medicine (Shanghai, China).

S. mutans was cultivated in tryptic soy broth (TSB) and agar (TSA). *F. nucleatum* and *P. gingivalis* were cultivated in brain heart infusion broth (BHI broth) and BHI agar with 0.0005% hemin, 0.0001% menadione and 5% defribrinated sheep blood. Culture temperature was maintained at 37 °C for each stains. *S. mutans*, *F. nucleatum* and *P. gingivalis* cells were incubated in anaerobic system (N_2 80%; H_2 10%; CO_2 10%).

Bacteria were harvested at the exponential growth phase. After cultures were centrifuged at 5000 rpm for 4 min, supernatant was discarded. Cells were washed at least two times with sterile isotonic saline. Bacterial cells were then resuspended in saline for the use of subsequent experiments.

2.3. 3-(4,5-Dimethylthiazol-2-yl)-2,5-diphenyl Tetrazolium Bromide (MTT) Reduction Assay. Utilization of 3-(4,5-dimethylthiazol-2-yl)-2,5-diphenyl tetrazolium bromide (MTT) would be a convenient assays for estimating cell metabolic activity.[16,17] 250 μL of diluted bacteria suspension that containing ~10^{10} CFU/mL was dispersed in microcentrifuge tubes and coincubated with GO (final concentration were 0, 20, 40, 80 μg/mL, respectively) for 2 h. At the end of incubation, 50 μL of MTT was added. After placing those tubes in dark for another 2 h, every tube was centrifuged at 10 000 rpm for 1 min and the supernatant was discarded. The precipitate containing formazan was dissolved in dimethyl sulfoxide (DMSO). Then the tubes were centrifuged one more time, and 200 μL of supernatant was trapped and transferred to a 96-well plate for analyzing using a microplate reader (Bio-Rad, USA). *S. mutans*, *F. nucleatum* and *P. gingivalis* were used in this assay. All the measurements were carried out at least three times.

2.4. Colony Forming Units (CFU) Counting Method. Bacterial cell suspensions were diluted to obtain cell samples containing 1 × 10^6 to 1 × 10^7 CFU/mL. In 1.5 mL microcentrifuge tubes, 250 μL of bacterium suspensions was mixed with a certain amount of 1 mg/mL GO and isotonic saline to ensure the final concentration of GO in each tube was 20, 40, 80 μg/mL, respectively. Isotonic saline solution without GO materials was served as control. Then, *S. mutans*, *F. nucleatum*, and *P. gingivalis* cells were incubated in anaerobic system at 37 °C for 2 h. With 10-fold series dilution, 100 μL of bacterial sample was plated onto Petri dishes. After the bacteria have had enough time and appropriate culture condition to incubate, colony counting method was applied to evaluate the viability of *S. mutans*, *F. nucleatum*, and *P. gingivalis*. All treatments were performed two times in triplicate.

2.5. Growth Curve Determination. The bacterial growth curves was studied by recording the change of turbidity of bacterial cultures through their life spans. 250 μL of bacterial suspension (containing 1 × 10^6 to 1 × 10^7 CFU/mL) that exposed to GO nanosheets for 2 h was added into 6 mL of fresh TSB/BHI medium. We set them in appropriate incubating system and measured the optical density at 600 nm by spectrophotometer (Shimadzu, Japan) at regular intervals until the bacteria growth reach a plateau. All treatments were performed two times in triplicate.

2.6. Live/Dead Fluorescent Staining. Bacterial cell suspensions were diluted to obtain cell samples containing 1 × 10^6 to 1 × 10^7 CFU/mL. In 1.5 mL microcentrifuge tubes, we mixed 250 μL of bacterium suspensions with 40 μL of 1 mg/mL GO and 210 μL of isotonic saline to ensure the final concentration of GO in tube was 80 μg/mL. Bacterial cells culture without GO nanosheets was served as control. *S. mutans*, *F. nucleatum*, and *P. gingivalis* cells were incubated in anaerobic box at 37 °C for 2 h. The Live/Dead BacLight Bacterial Viability Kits was utilized which is mixture of SYTO 9, a green-fluorescent live cells stain and propidium iodide (PI), a red-fluorescent dead cells stain. Same volume of SYTO 9 and PI were added to one clean microcentrifuge tube, respectively. After 2 h of incubation with

DOI: 10.1021/acsami.5b01069
ACS Appl. Mater. Interfaces 2015, 7, 5605−5611

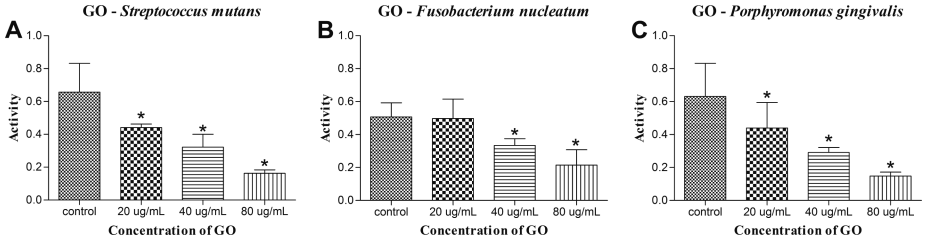

Figure 2. Antibacterial activity was evaluated by MTT assay. Bacteria were under the treatment of 20, 40, and 80 μg/mL GO at 37 °C for 2 h. The activities of (A) *S. mutans*, (B) *F. nucleatum*, and (C) *P. gingivalis* were represented by the ratio of $OD_{490\ nm}$ of GO-treated sample to that of samples before treatment. (* means p value <0.05).

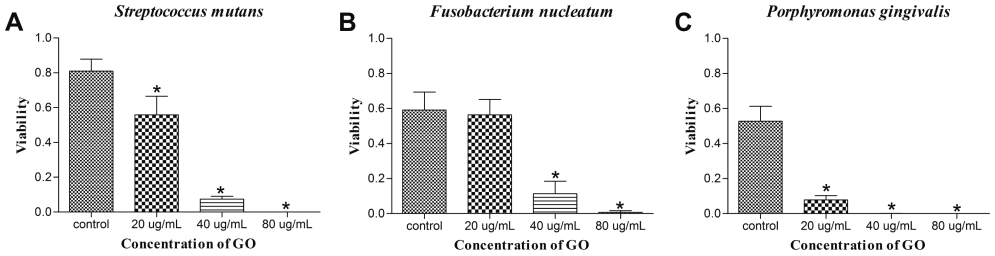

Figure 3. Colony forming units counting method was applied to evaluate the actual antimicrobial effect of GO nanosheets. With the treatment of 20, 40, and 80 μg/mL GO for 2 h, after 10-fold series dilution, (A) *S. mutans*, (B) *F. nucleatum*, and (C) *P. gingivalis* bacterial suspensions were plated onto Petri dishes, respectively. Bacteria treated with isotonic saline were used as control. Viability was calculated by the following formula: viability % = counts of samples after incubation with suspensions/counts of samples before incubation. (* means p value <0.05).

GO nanosheets, mixed the 1.5 μL of dye and 500 μL of samples thoroughly and incubated them at room temperature in the dark for 15 min. Five microliters of the stained bacterial suspension was trapped on an 18 mm square coverslip. We observed them in confocal laser scanning microscopy (CLSM, Leica TCS SP2, Germany). The excitation/emission of two dyes were 488/500−550 nm for the SYTO 9, and 488/590−680 nm for PI.

2.7. Transmission Electron Microscopy (TEM). The ~1 × 10^7 CFU mL *S. mutans* cells were suspended in GO nanosheets (80 μg/mL) and cultured at 37 °C for 4 h. The *S. mutans* cells were then fixed with 2% glutaraldehyde for 2 h at 4 °C. Cells were washed with phosphate buffer saline, fixed with 1% aqueous OsO_4 for 2 h, and washed again two times with PBS. Cells were then dehydrated via ethanol series (30%, 50% for 10 min, respectively), then 70% ethanol was applied for 18 h. Another ethanol series (80%, 95%, 100%) was applied for 10 min, respectively. Then embedded the samples in Epon/Araldite resin (polymerization at 60 °C for 48 h). Thin sections (90 nm) cut by ultra microtome were stained for 1 min each with 4% uranyl acetate (1:1 acetone/water) and 0.2% lead citrate, and examined under the transmission electron microscopy (PHILIP CM-120) .

2.8. Statistical Analysis. Data are presented as mean ± standard deviation. The values of experiment groups are compared to those of the control groups. Differences between two mean values were calculated by Student's t test. We consider the differences statistically significant if $p < 0.05$.

3. RESULTS AND DISCUSSION

3.1. Preparation and Characterization of GO. Graphene oxide nanosheets with a large amount of oxygen functional groups (hydroxyl carboxyl and epoxide groups) well dispersed in the water. Here, we synthesized GO nanosheets using the modified Hummers' method, which presented as a brown colloidal suspension. Atom force microscopy results showed that the thickness of GO nanosheets was about 1.0 nm, and the lateral dimensions of GO ranged from nanometers to micrometers (Figure 1A). Size of GO nanosheets would strongly influence their antibacterial activity. Larger sheets lead to more cell loss than smaller ones.[18] In our study, dynamic light scattering quantitatively revealed the size of 90% GO nanosheets distributed between 200 to 400 nm (Figure 1B). FTIR spectrum of GO displayed the stretching vibrations peak of C═O, C═C, C−O−C groups at 1728, 1625, and 1056 cm^{-1}, respectively (Figure 1C), which indicated the reservation of the sp^2 domains of carbon atoms and the presence of many oxygenated groups on the graphene sheets. Raman spectroscopy was utilized to investigate the carbon structure of graphite during the oxidation process. As shown in Figure 1D, our GO samples showed a typical Raman spectrum of graphene oxide (GO), with broad G and D band peaks at 1580 and 1350 cm^{-1}, respectively, and the intensity ratio of the D and G band (I_D/I_G) is 1.03. These characterizations confirmed that graphene oxide nanosheets had been successfully prepared.

3.2. Antimicrobial Effect of GO. MTT reduced assay was a convenient method to evaluate the activity of cells. MTT is a water-soluble yellow dye that can be reduced to water-insoluble purple formazan crystals by the dehydrogenase system of active cells. On the basis above theory, we can measure the optical density value of formazan at 490 nm to reveal the metabolic activity of live cells in culture.

To determine the effect of GO to *S. mutans*, GO was amended to samples containing 250 μL bacterial cell suspension with a final concentration of 20, 40, 80 μg/mL, respectively. After 2 h of incubation, we found the viability of *S. mutans* decreased along with the increasing GO concentration. Compared to origin status, the activity of bacterial cells was 44.2 ± 2.2, 32.2 ± 7.9, and 16.3 ± 2.1% when the concentration of GO was 20, 40, 80 μg/mL, respectively. At the same time, the activity of control was 65.7 ± 17.5%. (Figure 2A) As to *F. nucleatum* the activity of bacterial cells was 49.7 ± 11.8%, 33.4 ± 4.0%, 21.5 ± 9.4% when the concentration of GO was 20, 40, 80 μg/mL, respectively, and that of control was 50.7 ± 8.5%. (Figure 2B)For *P. gingivalis*, the activity of bacterial cells was 44.0 ± 15.5%, 29.1 ± 3.0%, 14.7 ± 2.5% when the concentration of GO was 20, 40, 80 μg/mL, respectively, and

DOI: 10.1021/acsami.5b01069
ACS Appl. Mater. Interfaces 2015, 7, 5605−5611

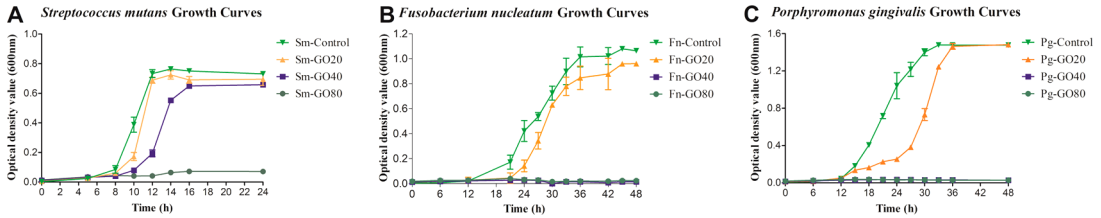

Figure 4. $OD_{600\ nm}$ growth curve of (A) *S. mutans*, (B) *F. nucleatum*, and (C) *P. gingivalis*, which were after treatment of GO nanosheets. The concentrations of GO were 20, 40, and 80 μg/mL, respectively. Bacteria treated with isotonic saline were used as control.

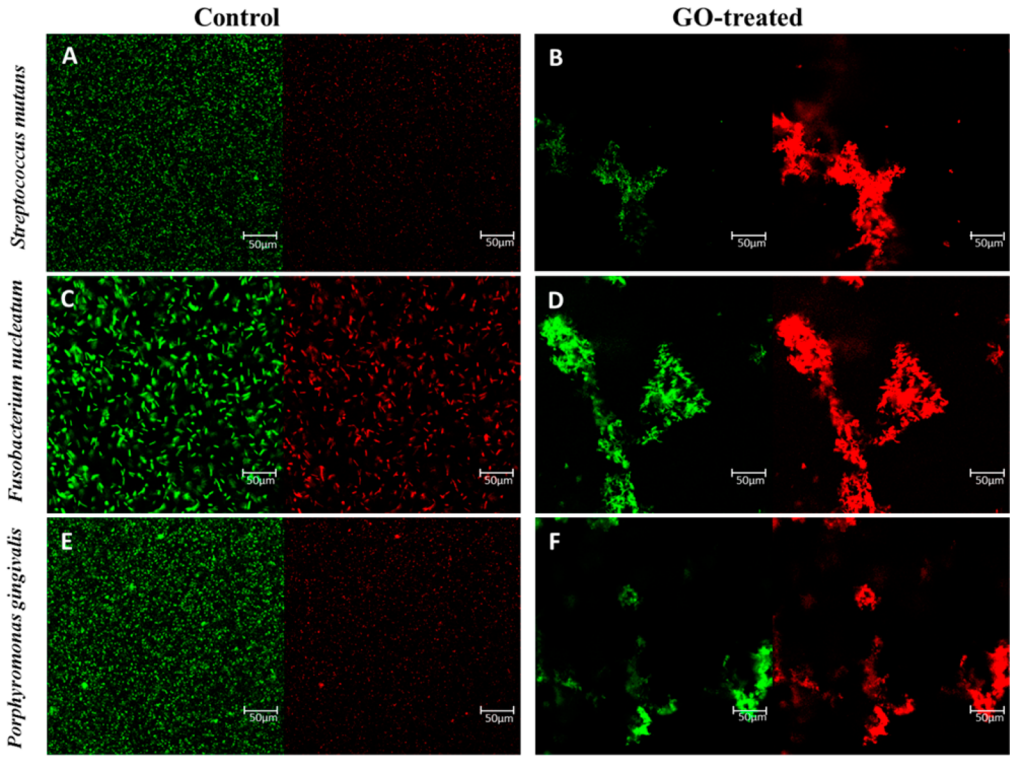

Figure 5. Live/dead fluorescent staining images. (A, B) *S. mutans*, (C, D) *F. nucleatum*, and (E, F) *P. gingivalis* cells were treated with GO nanosheets and isotonic saline (control) for 2 h. Representative fluorescence microscopy images of bacteria cells which were stained by SYTO 9 (green channel) and PI (red channel) for 15 min in dark. All treated cases had the same GO dose of 80 μg/mL. Scale bar = 50 μm.

that of control was 63. One ±20.1%. (Figure 2C) As for *S. mutans* and *P. gingivalis*, the differences between each GO-treated group and control were statistically significant. And *F. nucleatum* cells incubated with 40 μg/mL and more GO nanosheets decreased significantly.

Absolutely, the MTT reduced assay revealed the function of cells' dehydrogenase system. We then applied a classic colony forming units (CFUs) counting method to evaluate the actual antimicrobial effect of GO nanosheet against typical dental pathogens.

As to *S. mutans*, the viability came to 55.9 ± 10.7%, 7.5 ± 1.6%, ~0 ± 0% when the concentration of GO was 20, 40, 80 μg/mL, respectively (Figure 3A). At the same time, the viability of bacterial cells in saline came to 81.0 ± 6.9% that was higher than GO-treated groups. The differences between each GO-treated group and control were statistically significant. The similar situation occurred in *F. nucleatum* test. The viability were 56.4 ± 8.7%, 11.4 ± 7.1% and 0.8 ± 0.9% when the concentration of GO was 20, 40, 80 μg/mL, respectively (Figure 3B). Comparing to control (59.2 ± 10.2%), F. nucleatum cells with more than 40 μg/mL GO nanosheets were suppressed significantly. Similarly, as to *P. gingivalis* culture, the viability of control was 52.7 ± 8.5% and the GO-treated groups were 7.8 ± 2.4%, 0.1 ± 0.03% and ~0 ± 0% when the concentration of GO was 20, 40, 80 μg/mL, respectively (Figure 3C). The differences between each GO-treated group and control were statistically significant.

In this research, we found the viability of bacteria in control groups was as low as 81.0 ± 6.9%, 59.2 ± 10.2% and 52.7 ± 8.5%, for *S. mutans*, *F. nucleatum* and *P. gingivalis*, respectively. The reason for this phenomenon was that these three bacteria strains are oxygen susceptible, especially *P. gingivalis* and *F. nucleatum* which belong to strictly anaerobic bacteria. Therefore, *P. gingivalis* and *F. nucleatum* cannot survive normally or the viabilities of them decrease severely in oxygenated and carbon-dioxide-depleted environment.[19] Although we incubated *P. gingivalis* and *F. nucleatum* in anaerobic system, conventional concentrations of O_2 and CO_2 in atmosphere were difficult to be avoided when we diluted the sample and plated the culture onto Petri dishes.

GO-treated bacterial samples were added in fresh medium to be cultured. The optical density value at 600 nm represented the quantity of bacterial cells. Figure 4A revealed that *S. mutans* treated by GO of 80 μg/mL was killed absolutely and the

DOI: 10.1021/acsami.5b01069
ACS Appl. Mater. Interfaces 2015, 7, 5605−5611

medium remained clear in 24 h. Another two samples with GO concentrations of 40 and 20 μg/mL grew quite slower than the control. After the bacteria growth hit plateaus, we found the final quantity of bacteria decreased along with the increase of GO nanosheets concentration. In addition, there was a delay when GO-treated group turned into exponential phase that means GO nanosheets suppress largely the growth of bacteria. As to *F. nucleatum* (Figure 4B) and *P. gingivalis* (Figure 4C), when GO concentration came to 40 μg/mL, the bacterium cells stopped growing. The lag phases of *P. gingivalis* and *F. nucleatum* were prolonged to about 20 h which was quite long. In our research, the effect of GO nanosheets against obligate anaerobic bacteria is likely higher than facultative anaerobic bacteria. It may link to the differences of resistances against oxidative stress of anaerobic and facultative anaerobic bacteria. Oxidative stress is a highly recognized mechanism of various nanoparticles.[20] It is reported as a key mechanism for the antibacterial activity of graphene-based nanomaterials, such as GO, rGO nanosheets, fullerene, and carbon nanotubes (CNTs) through reactive oxygen species (ROS) generation.[20,21]

We performed bacterial live/dead fluorescent staining assays and observed with CLSM to identify the living status of bacteria cells. *S. mutans*, *F. nucleatum*, and *P. gingivalis* suspensions containing 1×10^6 to 1×10^7 CFU/mL cells were used. Then incubated them with 0, 20, 40, and 80 μg/mL GO nanosheets at 37 °C for 2 h. With an appropriate mixture of the SYTO 9 and propidium iodide stains, bacteria with intact cell membranes stain fluorescent green, whereas bacteria with damaged membranes stain fluorescent red. According to the figures obtained, homogeneous planktonic bacterial suspension aggregated after GO treated. According to Figure 5A, B, GO-treated *S. mutans* was more dead more than the control. This result means GO nanosheets induced the death of *S. mutans* cells, exactly. As to *F. nucleatum* (Figure 5C, D)and *P. gingivalis* (Figure 5E, F), we found similar results.

3.3. Morphology Change of Bacterial Cells after Exposure to GO. TEM analysis showed numbers of bacterial cells decreased in GO-treated groups comparing to control. We found GO nanosheets caused integrity loss of the cell membrane and cell wall based on TEM images. However, the cells in isotonic saline remained the normal shape and structure. With the surrounding of GO nanosheets (Figure 6, arrows a, d, and f), the intracellular densities of *S. mutans*, *F. nucleatum* and *P. gingivalis* decreased, revealing that they lost some intracellular substance (Figure 6, Arrow b and h). As to *P. gingivalis* cells, it was prominent that the cell wall and membrane were destroyed and inner cell structures leaked out severely. (Figure 6, arrow g) Furthermore, we found some *P. gingivalis* cell with all inner structures flowing out absolutely remaining a circle of cell wall. (Figure 6, arrow i) Particularly, GO-treated *F. nucleatum* images revealed the cell wall was stripped down (Figure 6, arrows c and e). As to *S. mutans* cells, slighter membrane damages occurred, and some damaged cells with an incomplete contour were also observed (Figure 6, arrow b). It was reported that the mechanism for the graphene-induced degradation of cell membranes includes by severe insertion and cutting and by destructive extraction of lipid molecules.[22] According to these TEM images, Gram-positive bacteria seemed to have stronger resistance against GO nanosheets compared to Gram-negative bacteria. However, previous studies reported that graphene nanowalls and single-walled carbon nanotubes (SWCNT) dispersions exhibit higher antibacterial activity against Gram-positive bacteria than Gram-negative bacteria. Gram-negative

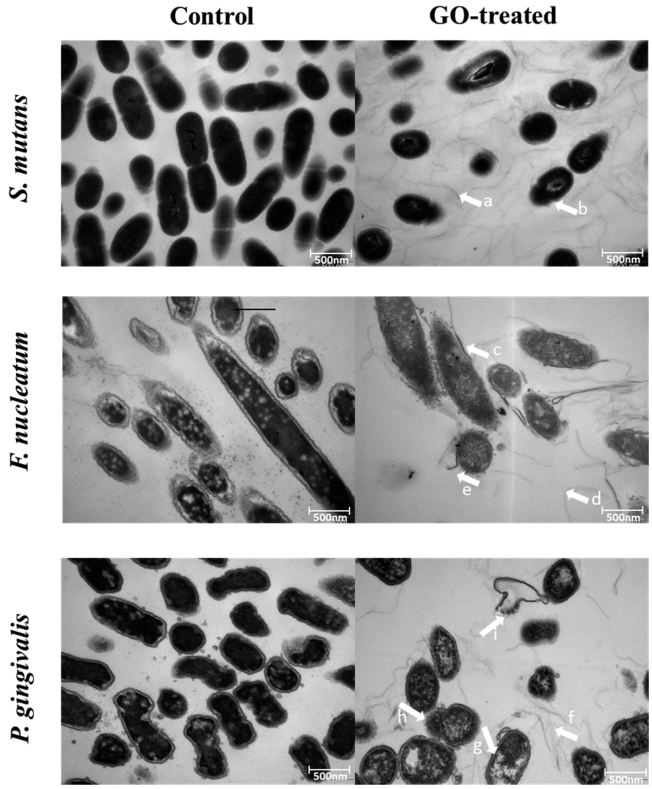

Figure 6. TEM images of *S. mutans*, *F. nucleatum*, and *P. gingivalis* cells after incubation with GO nanosheets dispersion (right side) for 2 h, and after incubation with saline solution for 2 h as control (left side). All treated cases had the same GO dose of 80 μg/mL. Scale bar = 500 nm.

bacteria have a complex outer membrane that may enhance the surface stiffness.[23,24] In addition, the differences among specific bacteria should be considered. This incompatible but interesting results need to be explored in future mechanism research.

In our research, TEM technique was utilized to observe the damage of cell wall and membrane, as well as the change of inner structure of cells. Related carbon nanomaterial such as SWCNT, fullerene and its derivatives exhibit strong antimicrobial activity through the direct contacting with bacteria membrane.[9,25,26] It has been reported that GO nanosheets can insert/cut through the cell membranes of bacteria cells and vigorously extract large amounts of phospholipids from the membranes.[22] GO nanosheets also can oxidize glutathione, which serves as redox state mediator in bacteria.[20] However, exact mechanisms after GO nanosheets cause the degradation of cell membrane are not clear. Metal oxide nanoparticals also have antibacterial activity.[27−30] Some metal oxide nanoparticle antibacterial research revealed that they directly contact with bacteria membrane, penetrate into the bacteria and interact with sulfur-containing protein as well as phosphorus-containing DNA. Then, the nanoparticles can disturb the respiratory chain and lead to bacterial cell death.[31−34] GO nanosheets, as another similar nanomaterial, the mechanical generality with nanoparticulate metals would be explored.

Most of dental caries, periapical, and periodontal diseases are directly caused by bacteria including, but not limited to *S. mutans*, *P. gingivalis*, and *F. nucleatum*.[35,36] In clinical practice, dentists use classic antibiotics, such as chlorhexidine, cephalosporin, metronidazole, tetracycline, etc. However,

DOI: 10.1021/acsami.5b01069
ACS Appl. Mater. Interfaces 2015, 7, 5605−5611

classic antibiotic families realize their antibacterial function by inhibition the synthesis of cell wall, protein, DNA, RNA, folic acid, etc. Drug resistance can be delivered to next generation by heredity.[37,38] With the abuse of antibiotics, we have to face the difficult situation called antibacterial drug resistance over the past decades.[39] These three dental pathogens can be killed by GO nanosheets directly as we found in TEM images. GO nanosheets, a new kind of antimicrobial material, decrease the possibility of the formation of drug resistance compared to classic antibiotics because of its physical mechanism. Notably, relatively convenient processing of GO with low cost provide the possibility for its wide application.

However, the oral cavity is a complex ecosystem including teeth, root canals, mucosa, periodontal tissues, saliva and dentures. Oral bacterial biofilm is the structure constituted by bacteria themselves and the substances produced or gathered by them. It exists on the surfaces of teeth, periodontal pockets, root canal systems, and dentures as a community.[40] It has been investigated that pure GO nanosheets have toxic effects to the development of mature biofilms from planktonic cells.[41] Bacterial biofilm has high pathogenicity because it is less susceptible to antibiotics but more resistant to physical offense.[42−44] Though GO nanosheets played an excellent role in killing planktonic pathogens and inhibiting the formation of bacterial biofilm, investigations on the activity of GO nanosheets against those pathogens within the context of an established biofilm are necessary.[41]

4. CONCLUSION

In conclusion, GO nanosheets were synthesized using modified Hummers' method. We studied the antimicrobial activity of GO nanosheets against common dental pathogens, such as *S. mutans*, *P. gingivalis* and *F. nucleatum*. It was revealed that the antimicrobial effect of GO nanosheets is prominent. With a higher concentration, GO nanosheets work more effective to suppress the viability of these dental pathogens. GO nanosheets can destroy the cell wall and membrane and make plasm leak out. GO nanosheets would be a kind of promising nanomaterial that can be applied in dental care and therapy.

AUTHOR INFORMATION

Corresponding Author

*E-mail: tangzisheng163@163.com (Zisheng Tang).

Author Contributions

†J.H. and X.Z. contributed equally.

Notes

The authors declare no competing financial interest.

ACKNOWLEDGMENTS

This work was financially supported by Shanghai Natural Science Foundation (13ZR1423900) and the Hospital-Public Cross-Link Project of Shanghai Jiao Tong University (YG2013MS58).

REFERENCES

(1) Wade, W. G. The Oral Mmicrobiome in Health and Disease. *Pharmacol. Res.* **2013**, *69*, 137−143.

(2) Loesche, W. J. Role of *Streptococcus mutans* in Human Dental Decay. *Microbiol. Rev.* **1986**, *50*, 353.

(3) Ximénez-Fyvie, L. A.; Haffajee, A. D.; Socransky, S. S. Comparison of the Microbiota of Supra-and Subgingival Plaque in Health and Periodontitis. *J. Clin. Periodontol.* **2000**, *27*, 648−657.

(4) Paster, B. J.; Boches, S. K.; Galvin, J. L.; Ericson, R. E.; Lau, C. N.; Levanos, V. A.; Sahasrabudhe, A.; Dewhirst, F. E. Bacterial Diversity in Human Subgingival Plaque. *J. Bacteriol.* **2001**, *183*, 3770−3783.

(5) Gomes, B.; Pinheiro, E.; Gadê-Neto, C.; Sousa, E.; Ferraz, C.; Zaia, A.; Teixeira, F.; Souza-Filho, F. Microbiological Examination of Infected Dental Root Canals. *Oral Microbiol. Immunol.* **2004**, *19*, 71−76.

(6) Novoselov, K. S.; Geim, A. K.; Morozov, S. V.; Jiang, D.; Zhang, Y.; Dubonos, S. V.; Grigorieva, I. V.; Firsov, A. A. Electric Field Effect in Atomically Thin Carbon Films. *Science* **2004**, *306*, 666−669.

(7) Geim, A. K.; Novoselov, K. S. The Rise of Graphene. *Nat. Mater.* **2007**, *6*, 183−191.

(8) Zhu, Y.; Murali, S.; Cai, W.; Li, X.; Suk, J. W.; Potts, J. R.; Ruoff, R. S. Graphene and Graphene Oxide: Synthesis, Properties, and Applications. *Adv. Mater.* **2010**, *22*, 3906−3924.

(9) Hu, W.; Peng, C.; Luo, W.; Lv, M.; Li, X.; Li, D.; Huang, Q.; Fan, C. Graphene-based Antibacterial Paper. *ACS Nano* **2010**, *4*, 4317−4323.

(10) Hui, L.; Piao, J.-G.; Auletta, J.; Hu, K.; Zhu, Y.; Meyer, T.; Liu, H.; Yang, L. Availability of the Basal Planes of Graphene Oxide Determines whether it is Antibacterial. *ACS Appl. Mater. Interfaces* **2014**, *6*, 13183−13190.

(11) Krishna, K. V.; Ménard-Moyon, C.; Verma, S.; Bianco, A. Graphene-based Nanomaterials for Nanobiotechnology and Biomedical Applications. *Nanomedicine* **2013**, *8*, 1669−1688.

(12) Zhao, J.; Deng, B.; Lv, M.; Li, J.; Zhang, Y.; Jiang, H.; Peng, C.; Li, J.; Shi, J.; Huang, Q.; Fan, C. Graphene Oxide-based Antibacterial Cotton Fabrics. *Adv. Healthcare Mater.* **2013**, *2*, 1259−1266.

(13) Kulshrestha, S.; Khan, S.; Meena, R.; Singh, B. R.; Khan, A. U. A Graphene/zinc Oxide Nanocomposite Film Protects Dental Implant Surfaces Against Cariogenic *Streptococcus mutans*. *Biofouling* **2014**, *30*, 1281−1294.

(14) Hummers, W. S., Jr; Offeman, R. E. Preparation of Graphitic Oxide. *J. Am. Chem. Soc.* **1958**, *80*, 1339−1339.

(15) Zhang, H.; Peng, C.; Yang, J.; Lv, M.; Liu, R.; He, D.; Fan, C.; Huang, Q. Uniform Ultrasmall Graphene Oxide Nanosheets with Low Cytotoxicity and High Cellular Uptake. *ACS Appl. Mater. Interfaces* **2013**, *5*, 1761−1767.

(16) Carmichael, J.; DeGraff, W. G.; Gazdar, A. F.; Minna, J. D.; Mitchell, J. B. Evaluation of a Tetrazolium-based Semiautomated Colorimetric Assay: Assessment of Chemosensitivity Testing. *Cancer Res.* **1987**, *47*, 936−942.

(17) Wang, H.; Cheng, H.; Wang, F.; Wei, D.; Wang, X. An Improved 3-(4,5-dimethylthiazol-2-yl)-2,5-diphenyl Tetrazolium Bromide (MTT) Reduction Assay for Evaluating the Viability of *Escherichia coli* cells. *J. Microbiol. Methods* **2010**, *82*, 330−333.

(18) Liu, S.; Hu, M.; Zeng, T. H.; Wu, R.; Jiang, R.; Wei, J.; Wang, L.; Kong, J.; Chen, Y. Lateral Dimension-dependent Antibacterial Activity of Graphene Oxide Sheets. *Langmuir* **2012**, *28*, 12364−12372.

(19) Diaz, P.; Zilm, P. S.; Rogers, A. H. *Fusobacterium nucleatum* Supports the Growth of *Porphyromonas gingivalis* in Oxygenated and Carbon-dioxide-depleted Environments. *Microbiology* **2002**, *148*, 467−472.

(20) Liu, S.; Zeng, T. H.; Hofmann, M.; Burcombe, E.; Wei, J.; Jiang, R.; Kong, J.; Chen, Y. Antibacterial Activity of Graphite, Graphite Oxide, Graphene Oxide, and Reduced Graphene Oxide: Membrane and Oxidative Stress. *ACS Nano* **2011**, *5*, 6971−6980.

(21) Gurunathan, S.; Han, J. W.; Dayem, A. A.; Eppakayala, V.; Kim, J. H. Oxidative Stress-mediated Antibacterial Activity of Graphene Oxide and Reduced Graphene Oxide in *Pseudomonas aeruginosa*. *Int. J. Nanomed.* **2012**, *7*, 5901−5914.

(22) Tu, Y.; Lv, M.; Xiu, P.; Huynh, T.; Zhang, M.; Castelli, M.; Liu, Z.; Huang, Q.; Fan, C.; Fang, H. Destructive Extraction of Phospholipids from *Escherichia coli* Membranes by Graphene Nanosheets. *Nat. Nanotechnol.* **2013**, *8*, 594−601.

(23) Akhavan, O.; Ghaderi, E. Toxicity of Graphene and Graphene Oxide Nanowalls Against Bacteria. *ACS Nano* **2010**, *4*, 5731−5736.

(24) Liu, S.; Wei, L.; Hao, L.; Fang, N.; Chang, M. W.; Xu, R.; Yang, Y.; Chen, Y. Sharper and Faster "Nano Darts" Kill More Bacteria: A

DOI: 10.1021/acsami.5b01069
ACS Appl. Mater. Interfaces 2015, 7, 5605−5611

Study of Antibacterial Activity of Individually Dispersed Pristine Single-walled Carbon Nanotube. *ACS Nano* **2009**, *3*, 3891−3902.
(25) Kang, S.; Pinault, M.; Pfefferle, L. D.; Elimelech, M. Single-walled Carbon Nanotubes Exhibit Strong Antimicrobial Activity. *Langmuir* **2007**, *23*, 8670−8673.
(26) Tang, Y. J.; Ashcroft, J. M.; Chen, D.; Min, G.; Kim, C.-H.; Murkhejee, B.; Larabell, C.; Keasling, J. D.; Chen, F. F. Charge-associated Effects of Fullerene Derivatives on Microbial Structural Integrity and Central Metabolism. *Nano Lett.* **2007**, *7*, 754−760.
(27) Hernandez-Sierra, J. F.; Ruiz, F.; Pena, D. C.; Martinez-Gutierrez, F.; Martinez, A. E.; Guillen Ade, J.; Tapia-Perez, H.; Castanon, G. M. The Antimicrobial Sensitivity of *Streptococcus mutans* to Nanoparticles of Silver, Zinc Oxide, and Gold. *Nanomedicine* **2008**, *4*, 237−240.
(28) Liu, Y.; He, L.; Mustapha, A.; Li, H.; Hu, Z. Q.; Lin, M. Antibacterial Activities of Zinc Oxide Nanoparticles Against *Escherichia coli* O157:H7. *J. Appl. Microbiol.* **2009**, *107*, 1193−1201.
(29) Xie, Y.; He, Y.; Irwin, P. L.; Jin, T.; Shi, X. Antibacterial Activity and Mechanism of Action of Zinc Oxide Nanoparticles Against *Campylobacter jejuni*. *Appl. Environ. Microbiol.* **2011**, *77*, 2325−2331.
(30) Chatterjee, T.; Chatterjee, B. K.; Majumdar, D.; Chakrabarti, P. Antibacterial Effect of Silver Nanoparticles and the Modeling of Bacterial Growth Kinetics Using a Modified Gompertz Model. *Biochim. Biophys. Acta* **2015**, *1850*, 299−306.
(31) Nel, A.; Xia, T.; Madler, L.; Li, N. Toxic Potential of Materials at the Nanolevel. *Science* **2006**, *311*, 622−627.
(32) Li, W.-R.; Xie, X.-B.; Shi, Q.-S.; Zeng, H.-Y.; You-Sheng, O.-Y.; Chen, Y.-B. Antibacterial Activity and Mechanism of Silver Nanoparticles on *Escherichia coli*. *Appl. Microbiol. Biotechnol.* **2010**, *85*, 1115−1122.
(33) Rai, M.; Yadav, A.; Gade, A. Silver Nanoparticles as a New Generation of Antimicrobials. *Biotechnol. Adv.* **2009**, *27*, 76−83.
(34) Zarei, M.; Jamnejad, A.; Khajehali, E. Antibacterial Effect of Silver Nanoparticles Against Four Foodborne Pathogens. *Jundishapur J. Microb.* **2014**, *7*, e8720.
(35) Dewhirst, F. E.; Chen, T.; Izard, J.; Paster, B. J.; Tanner, A. C.; Yu, W.-H.; Lakshmanan, A.; Wade, W. G. The Human Oral Microbiome. *J. Bacteriol.* **2010**, *192*, 5002−5017.
(36) Chen, T.; Yu, W.-H.; Izard, J.; Baranova, O. V.; Lakshmanan, A.; Dewhirst, F. E. The Human Oral Microbiome Database: a Web Accessible Resource for Investigating Oral Microbe Taxonomic and Genomic Information. *Database* **2010**, baq013.
(37) Walsh, C. Molecular Mechanisms that Confer Antibacterial Drug Resistance. *Nature* **2000**, *406*, 775−781.
(38) Levy, S. B.; Marshall, B. Antibacterial Resistance Worldwide: Causes, Challenges and Responses. *Nat. Med.* **2004**, *10*, S122−S129.
(39) Pallasch, T. Global Antibiotic Resistance and its Impact on the Dental Community. *J. Calif. Dent. Assoc.* **2000**, *28*, 215−233.
(40) Marsh, P. Dental Plaque: Biological Significance of a Biofilm and Community Life-style. *J. Clin. Periodontol.* **2005**, *32*, 7−15.
(41) Carpio, I. E. M.; Santos, C. M.; Wei, X.; Rodrigues, D. F. Toxicity of a Polymer−graphene oxide Composite Against Bacterial Planktonic Cells, Biofilms, and Mammalian Cells. *Nanoscale* **2012**, *4*, 4746−4756.
(42) Struzycka, I. The Oral Microbiome in Dental Caries. *Polym. J. Microbiol.* **2014**, *63*, 127−135.
(43) Davies, D. Understanding Biofilm Resistance to Antibacterial Agents. *Nat. Rev. Drug Discovery* **2003**, *2*, 114−122.
(44) Allaker, R. P.; Memarzadeh, K. Nanoparticles and the Control of Oral Infections. *Int. J. Antimicrob. Agents* **2014**, *43*, 95−104.

DOI: 10.1021/acsami.5b01069
ACS Appl. Mater. Interfaces 2015, 7, 5605−5611